Fe-bearing trioctahedral micas from Mont Saint-Hilaire, Québec, Canada

A. E. LALONDE

Department of Geology, Ottawa-Carleton Geoscience Center, University of Ottawa, Ottawa, Ontario, K1N 6N5, Canada

D. G. RANCOURT

Department of Physics, Ottawa-Carleton Geoscience Center, University of Ottawa, Ottawa, Ontario, K1N 6N5, Canada

AND

G. Y. CHAO

Department of Earth Sciences, Ottawa-Carleton Geoscience Center, Carleton University, Ottawa, Ontario, K1H 5P6, Canada

Abstract

We document the occurrence of Fe-bearing trioctahedral micas in the Poudrette quarry in the Mont Saint-Hilaire alkaline intrusion, characterize them by microprobe analysis, Mössbauer spectroscopy, X-ray diffraction, and optical measurements, describe their mineral chemistry, and discuss their petrological significance. In the nepheline and sodalite syenite, biotite and annite occur as coarse crystals characterized by low Al content (typically 2 atoms per formula unit, a.f.u.), high Mn content (typically 0.2 to 0.8 a.f.u.) and variable Fe/(Fe+Mg) values from 0.61 to 0.97. In the gabbro, biotite is less Fe-rich, has lower Mn content and high Ti content. Phlogopite is found as small metamorphic crystals in marble xenoliths within the syenite and siderophyllite occurs as large crystals in a metasomatized albitite dyke. Fe^{3+}/Fe_{tot} values extend from 0.079 in the siderophyllite to 0.282 in a high-Fe^{3+} annite. All of the micas except for the phlogopite have high contents of $(Fe^{3+})^{iv}$ ($\sim$0.13 to 0.45 a.f.u.) despite the high availability of Al in the rocks. We suggest that the high $(Fe^{3+})^{iv}$ amounts are caused by the high Mn abundance via a local structural mechanism. The great variety of mica encountered at Mont Saint-Hilaire reflects the highly heterogeneous conditions that prevailed during magmatic and postmagmatic crystallization in this intrusion.

KEYWORDS: biotite, phlogopite, annite, siderophyllite, mineral chemistry, Mössbauer spectroscopy, Mont Saint-Hilaire, Canada.

Geological setting

MONT SAINT-HILAIRE is a prominent roughly circular hill approximately 3 km in diameter that rises abruptly from the St-Lawrence lowlands just to the east of Montréal in the Province of Québec. The hill is a member of the Early Cretaceous Monteregian Hills (Adams, 1903), an alkaline petrographical province that includes ten separate intrusions arranged in a linear array extending approximately 235 km from Oka just west of Montréal to the Québec–Maine border in the east (Fig. 1).

The Mont Saint-Hilaire intrusion is composed of an older western half of alkaline gabbro and associated mafic rocks and an eastern half of peralkaline nepheline syenite and associated igneous breccia. Currie *et al.* (1986) recognized three suites: (1) the Sunrise suite composed of layered alkaline gabbro; (2) the Pain de Sucre suite which is composed of nepheline gabbro, diorite, and monzonite; and (3) the East Hill suite composed of peralkaline nepheline syenite, porphyry and associated igneous breccias. A thin biotite-grade hornfels occurs in the undeformed shale, siltstone and

Mineralogical Magazine, June 1996, Vol. 60, pp. 447–460

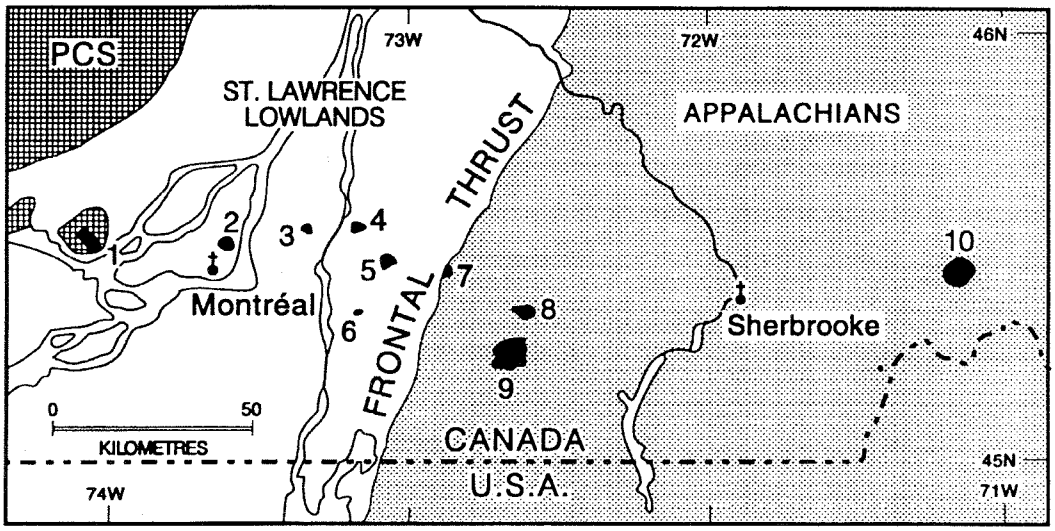

FIG. 1. Location of Mont Saint-Hilaire with respect to Montréal and the other Monteregian intrusions (after Gold, 1967). Index: (1) Oka carbonatite, (2) Mont-Royal, (3) Saint-Bruno, (4) Saint-Hilaire, (5) Rougemont, (6) Saint-Grégoire, (7) Yamaska, (8) Shefford, (9) Brome and (10) Mégantic, PCS represents the Precambrian Shield.

limestone host-rocks of the Ordovician Lorraine and Richmond groups (Currie *et al.*, 1986). The complex has been repeatedly dated by numerous radiochronological methods including Rb-Sr (Fairbairn *et al.* 1963), fission-track (Currie *et al.*, 1986), and K-Ar and $^{40}Ar/^{39}Ar$ (Gilbert and Foland, 1986). All the reported ages are Cretaceous and are centred around 125 Ma.

Mont Saint-Hilaire is well known as a mineral locality. As of spring 1994, this locality boasted of the occurrence of 299 mineral species, 27 of which were new minerals (Chao, pers. comm., 1994). All the minerals were found in the Poudrette quarry excavated within the rocks of the East Hill suite on the northeast side of the intrusion. Many of these mineral species result from enrichments in incompatible elements such as the rare-earths, zirconium, or manganese in the magmas and associated fluids. Several excellent reviews of the mineralogy of Mont Saint-Hilaire have been written including those by Mandarino and Anderson (1989), and Horváth and Gault (1990).

Although the dominant rock types of the East Hill suite are nepheline syenite and sodalite syenite, a wide variety of rock types is found in the quarry and reflects the heterogeneous physico-chemical conditions under which crystallization took place. This variety of rock types includes pegmatites, marble xenoliths, sodalite syenite, nepheline syenite, hornfels, igneous breccias and sodalite syenite xenoliths. The great diversity in mineral species encountered at Mont Saint-Hilaire is often believed to reflect the multitude of complex and isolated petrological environments.

Not surprisingly, the composition of the Fe-bearing trioctahedral micas at Mont Saint-Hilaire mimics the enormous heterogeneity that is observed in the rocks. To illustrate this we find in a radius of a few hundred metres micas ranging in Fe/(Fe+Mg) composition from phlogopite to nearly pure end-member annite and in total aluminum contents from Al-depleted micas to siderophyllite. In addition, many specimens have enrichments in Ti or Mn that can be linked to specific rock units.

Occurrence of micas

This study is based on eight specimens of Fe-bearing trioctahedral mica that were collected within the Poudrette quarry at Mont Saint-Hilaire. They are presented in order of increasing Fe/(Fe+Mg) in Table 1 and are labelled with the mineral symbols of Kretz (1983) (we suggest the symbol Sdp for siderophyllite). The specimens include a phlogopite (Phl) in the sense of Deer *et al.* (1962) (i.e. Fe/(Fe+Mg) < 0.33), four biotites (Bt-a, -b, -c and -d), an Fe^{3+}-rich annite (Ann-x), a regular (i.e. less Fe^{3+}-rich) annite (Ann) and one siderophyllite (Sdp). All specimens except for Bt-c were collected by one of us (G.Y.C.). Specimen Bt-c is from the collection of

TABLE 1. Composition of phlogopite, biotite, annite and siderophyllite from Mont Saint-Hilaire

Sample	Phl	Bt-a	Bt-b	Bt-c	Bt-d	Ann-x	Ann	Sdp
Component oxides (wt.%)								
SiO_2	41.26	35.67	37.22	38.67	34.28	33.25	33.82	30.29
TiO_2	0.14	7.22	2.54	2.53	1.07	1.49	1.25	0.26
Al_2O_3	10.44	13.75	10.03	9.33	8.74	10.93	9.95	21.55
Cr_2O_3								0.05
Fe_2O_3			3.22	3.39	5.49	11.47	7.59	2.69
FeO	13.46[1]	17.06[1]	21.03	21.72	24.47	26.27	32.18	28.27
MnO	0.32	0.24	2.10	1.75	5.19	1.86	2.47	1.71
MgO	18.21	11.95	8.47	8.54	4.54	0.63	0.59	0.44
CaO				0	0.01	0.02	0	0.01
Na_2O	0.20	0.43	0.24	0.22	0.22	0.40	0.46	0.25
K_2O	9.64	8.96	8.96	9.41	7.74	7.64	8.78	8.48
H_2O[2]	2.44	3.73	2.74	2.78	2.98	3.42	3.28	3.48
F	3.27	0.46	2.20	2.04	1.35	0.45	0.56	0.41
Cl	0.04	0.07	0.02	0.22	0.01	0.03	0.03	0.17
O≡F, Cl	−1.39	−0.21	−0.94	−0.91	−0.57	−0.20	−0.25	−0.21
Total	98.03	99.33	97.83	99.69	95.52	97.66	100.71	97.85
Mineral formulae based on 22 oxygens								
Si^{4+}	6.209	5.415	5.953	6.075	5.864	5.594	5.653	4.984
Al^{3+}	1.791	2.460	1.806	1.709	1.686	2.166	1.959	2.873
Fe^{3+}	0	0.125[3]	0.241	0.216	0.450	0.240[3]	0.388	0.143
ΣTet.	8	8	8	8	8	8	8	8
Al^{3+}	0.060	0	0.084	0.019	0.076	0	0.002	1.314
Ti^{4+}	0.015	0.824	0.305	0.298	0.137	0.188	0.158	0.033
Cr^{3+}								0.006
Fe^{3+}			0.147	0.184	0.257	1.212	0.567	0.191
Fe^{2+}	1.694	2.041	2.813	2.853	3.501	3.696	4.499	3.897
Mn^{2+}	0.041	0.031	0.284	0.232	0.752	0.264	0.350	0.239
Mg^{2+}	4.085	2.704	2.021	2.000	1.159	0.159	0.147	0.107
ΣOct.	5.896	5.600	5.653	5.586	5.882	5.520	5.723	5.787
Ca^{2+}				0	0.002	0.004	0	0.001
Na^{+}	0.058	0.127	0.073	0.065	0.072	0.129	0.150	0.080
K^{+}	1.851	1.735	1.827	1.885	1.689	1.640	1.873	1.784
ΣInt.	1.909	1.862	1.901	1.951	1.764	1.774	2.022	1.865
OH^{-}	2.434	3.761	2.882	2.928	3.266	3.753	3.694	3.743
F^{-}	1.556	0.221	1.113	1.014	0.732	0.239	0.296	0.211
Cl^{-}	0.010	0.018	0.005	0.059	0.002	0.008	0.010	0.046
Fe/(Fe+Mg)	0.293	0.445	0.613	0.619	0.784	0.970	0.974	0.975
Fe^{3+}/Fe_{tot}			0.121	0.123	0.168	0.282	0.175	0.079
$(Fe^{3+})^{iv}/Fe_{tot}$		0.058[3]	0.075	0.066	0.107	0.047[3]	0.071	0.034

[1] Total Fe expressed as FeO
[2] H_2O calculated from stoichiometry, i.e. assuming that OH+F+Cl = 4
[3] $(Fe^{3+})^{iv}$ not measured by Mössbauer spectroscopy but required to fill T to 8.

the Royal Ontario Museum and was collected by museum staff (ROM collection number M29662). Specimen Ann has also been deposited at the Royal Ontario Museum (ROM collection number M42126). Its magnetism investigated by magnetometry and low-temperature Mössbauer spectroscopy has been reported (Rancourt *et al.*, 1994*a*) and its room temperature Fe^{2+} quadrupole splitting distribution

TABLE 2. Optical properties and cell parameters of biotite, annite and siderophyllite from Mont Saint-Hilaire

Sample	Bt-a	Bt-b	Bt-c	Bt-d	Ann	Ann-x	Sdp
Optical properties							
Refractive indices[1]							
α				1.600	1.613	1.625	1.600
β				1.663	1.679	?[2]	1.657
γ				1.663	1.679	?[2]	1.657
$2V_\alpha$				12°	11°		11°
Dispersion				r<v	r<v		r<v
Pleochroism[3]							
α		drk rd-br		rd-br	org-br	rd-br	rd-br
β	drk rd-br	br		olv-gr	olv-gr	drk olv-gr	olv-gr
γ	drk rd-br	br		olv-gr	olv-gr	drk olv-gr	olv-gr
Unit cell parameters							
a		5.363(2)	5.361(3)	5.384(2)	5.419(2)	5.393(2)	5.386(1)
b		9.290(3)	9.276(6)	9.321(5)	9.384(6)	9.340(6)	9.323(6)
c		10.242(3)	10.240(5)	10.290(5)	10.341(8)	10.311(7)	10.256(7)
β		100.12(3)	100.14(5)	100.13(5)	100.30(3)	100.16(3)	100.10(3)
Volume		502.3(2)	501.2(4)	508.3(4)	517.4(7)	511.3(7)	507.0(7)

[1] Measurements at λ = 589.3 nm.
[2] Strong absorption prevents measurement.
[3] Colour abbreviations: br, brown; drk, dark; gr, green; olv, olive; org, orange; rd, reddish.

(QSD) has been compared to the QSDs of related synthetic micas (Rancourt *et al.*, 1994*b*). Brief descriptions of the physical properties and mode of occurrence of the specimens follow.

Phlogopite. Specimen Phl consists of small euhedral to subhedral black crystals that are typically ⩽1 mm across. They are found as accessory minerals in a pale green marble xenolith composed principally of diopside with calcite and pectolite, that is found within the nepheline syenite.

Biotite. Specimen Bt-a consist of very small (⩽3 mm across) anhedral crystals with a black colour and a brownish lustre that occur along with titanian augite in a xenolith of foliated gabbro found within the nepheline syenite. In this gabbro, the biotite and pyroxene are interstitial to euhedral plagioclase laths up to 3 cm in length. Specimens Bt-b and -c occur as small euhedral to subhedral black crystals 0.5 to 1.5 cm across in a granular micaceous rock associated with nepheline syenite. Specimen Bt-d consists of small euhedral to subhedral black crystals typically 1 to 4 mm across that occur in a dark, micaceous granular rock associated with potassium feldspar and albite. This rock was found as irregular elongated zones on two levels of the quarry and is probably a remobilized syenite dyke.

Annite. Specimen Ann-x occurs as unusual bladed crystals up to 4 cm long in a nepheline syenite dyke composed of microcline, nepheline, aegirine and accessory eudialyte. The strange bladed habit of these crystals results from the preferential development of {010}. Specimen Ann occurs in nepheline syenite as black euhedral to subhedral crystals with good hexagonal outlines that can be up to 6 cm across and 2 cm in thickness.

Siderophyllite. Specimen Sdp is found as large black crystals that are subhedral to anhedral and up to 2.5 cm across in a chalky-white fine-grained almost aphanitic rock. This rock is composed almost exclusively of albite with, in addition to siderophyllite, trace amounts of dawsonite, siderite, pyrite, allanite-(Ce), muscovite, apatite and analcime. The rock is believed to be a highly metasomatized albitite dyke.

Refractive indices, optical properties and unit-cell parameters of representative specimens are included in Table 2.

Analytical techniques

Most mineral analyses were obtained by wavelength-dispersive X-ray spectrometry using the Camebax electron microprobe of the McGill University Microprobe Laboratory. Typical beam operating conditions were 15 kV and 20 nA. ZAF data reduction was performed with the on-board Cameca

software. Other analyses were obtained with the Cambridge Microscan 5 microprobe of Carleton University. Here also, data were acquired in wavelength-dispersive mode under similar beam operating conditions.

Optical parameters were obtained from single crystals oriented with a goniometer head mounted on a spindle stage. Refractive indices were determined by immersion methods under sodium light (λ = 589.3 nm).

Unit-cell parameters were refined from X-ray powder diffraction patterns taken on a 114.6 mm Gandolfi camera with Co-$K\alpha$ radiation using an IBM-PC version of the Appleman and Evans least-squares refinement program (1973). Indexing was accomplished by comparing intensities with single-crystal precession photographs.

The values of Fe^{3+}/Fe_{tot}, $(Fe^{3+})^{iv}/Fe_{tot}$ and $(Fe^{3+})^{vi}/Fe_{tot}$ were determined by transmission Mössbauer spectroscopy. Spectra were taken with a ^{57}Co rhodium matrix source with both source and absorber at room temperature (22°C). The transducer was operated in constant acceleration mode. Data were accumulated in 1024 channels, which covered twice the Doppler velocity range of $\pm$4.0 mm/s. Calibration spectra were obtained with an ^{57}Fe-enriched iron foil either before or after each experiment. All positions are given with respect to this calibration spectrum (i.e. with respect to the centre shift of α-Fe at room temperature). All spectra were folded to obtain flat background profiles and are presented on a velocity scale of -2.5 to $+4.0$ mm/s. In all spectra, the signal to noise ratio is greater than 100.

Absorbers for the Mössbauer experiments were prepared from flakes that were cleaved from larger single crystals. All flakes were examined under binocular and polarising microscopes to ensure that no other mineral phases were present before being powdered or granulated in either ethanol or acetone to prevent oxidation. The powdered or granulated mica was then suspended in a 6 mm-thick, 0.5 inch dia. petroleum jelly mount. This method ensures that the orientation of crystal fragments in the absorbers is sufficiently random to impose equality in area of corresponding high and low-energy lines from the site-specific doublets (Rancourt, 1994*a*). The mass of sample used in the absorbers varied between 24 and 100 mg and, when sample availability permitted, was determined by the method of Rancourt *et al.* (1993) to maximize the signal to noise ratio.

The principal cause of spectral line broadening in the room temperature Mössbauer spectra of micas is known to be quadrupole splitting distributions (QSDs) that arise from the local structural disorder associated with cation disorder in the octahedral and tetrahedral sheets (Rancourt, 1994*a*, *b*, Rancourt *et al.*, 1994*b*). It is therefore incorrect to fit the spectra with Lorentzian lines whose widths are allowed to be significantly greater than the natural linewidth in order to account for the disorder (or inhomogeneous) broadening. This is because the Lorentzian lineshape itself is incorrect in such an application. A Lorentzian of the correct width will have overly large wings. One should fit with actual QSDs.

We use the new Voigt-based method of arbitrary-shape QSDs of Rancourt and Ping (1991) to fit the spectra. It allows one to assume that the true underlying QSD for a given valence state and coordination number (i.e. for a given 'site') is composed of a given number N of Gaussian components. Only as many Gaussian components as can be justified on statistical grounds are used and unique distributions are thereby obtained (Rancourt and Ping, 1991).

Even with correct QSD analysis, many factors affect the site populations obtained by Mössbauer spectroscopy. These have been reviewed by Rancourt (1989). The main error in the populations Fe^{2+}/Fe_{tot}, $(Fe^{3+})^{vi}/Fe_{tot}$ and $(Fe^{3+})^{iv}/Fe_{tot}$ arises from spectral area tradeoffs between neighbouring (and overlapping) lines (Rancourt *et al.*, 1994*c*). We have determined this error by mapping out the regions of statistically-equivalent fits in the space of the three relevant populations. In this way, Fe^{2+}/Fe_{tot} is found to have a well-defined value for each spectrum because the high-energy Fe^{2+} spectral lines produce an absorption line that is well separated from the rest of the spectrum. On the other hand, the $(Fe^{3+})^{vi}$ and $(Fe^{3+})^{iv}$ areas trade off significantly thereby causing the relatively large quoted errors in $(Fe^{3+})^{vi}/Fe_{tot}$ and $(Fe^{3+})^{iv}/Fe_{tot}$ (see Table 3).

TABLE 3. Oxidation and coordination states of iron in biotite, annite and siderophyllite from Mont Saint-Hilaire

	Fe^{3+}/Fe_{tot}	$(Fe^{3+})^{iv}/Fe_{tot}$	$(Fe^{3+})^{iv}/Fe_{tot}$ from site assignments
Bt-b	$0.121^{+0.001}_{-0.001}$	$0.075^{+0.012}_{-0.016}$	0.049
Bt-c	$0.123^{+0.002}_{-0.002}$	$0.066^{+0.002}_{-0.002}$	0.061
Bt-d	0.168	0.107	0.089
Ann	$0.175^{+0.004}_{-0.005}$	$0.071^{+0.008}_{-0.018}$	0.071
Ann-x	0.282	?[1]	0.047
Sdp	0.079	0.034	?[2]

[1] Impossible to resolve, spectral contribution of $(Fe^{3+})^{iv}$ is completely overlapped by $(Fe^{3+})^{vi}$.

[2] Sufficient Al to fill T to 8.

Mössbauer results

Mössbauer spectra for specimens Bt-b, -c, -d, Ann, -x and Sdp are presented in Fig. 2. All spectra were analysed for total Fe^{3+} and Fe^{2+}; in addition, the distribution of Fe^{3+} between tetrahedral and octahedral sites was evaluated for all specimens excluding Ann-x, where the high abundance of $(Fe^{3+})^{vi}$ made it impossible to resolve the spectral contribution from $(Fe^{3+})^{iv}$ (Table 3). Errors associated with the fitting of the spectra were evaluated for specimens Ann, Bt-b, and -c (Table 3).

All spectra show remarkable similarity and have three main absorption peaks centred at ≈ -0.1, +1.0 and +2.3 mm/s. These three peaks correspond respectively with (1) the sum of low-energy lines from $(Fe^{2+})^{vi}$ and $(Fe^{3+})^{vi}$ doublets; (2) the high-energy lines from $(Fe^{3+})^{vi}$ doublets; and (3) the high-energy lines from $(Fe^{2+})^{vi}$ doublets. In addition, all spectra except for Ann-x show a pronounced shoulder at ≈ 0.4 mm/s corresponding with the high-energy line of $(Fe^{3+})^{iv}$ doublets (Rancourt *et al.*, 1992).

In all spectra, the $(Fe^{2+})^{vi}$ contributions were modelled by QSDs that were assumed to be sums

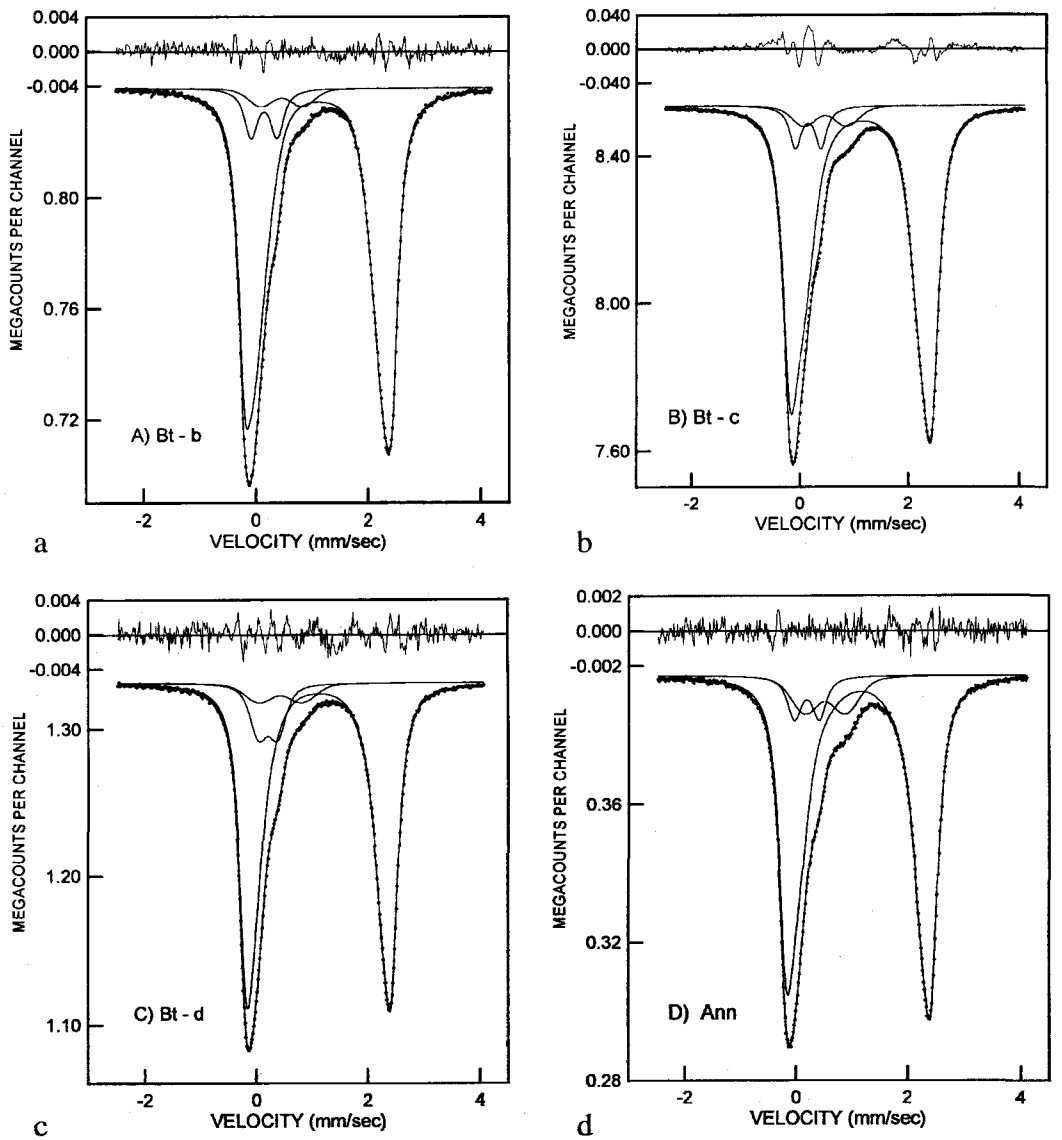

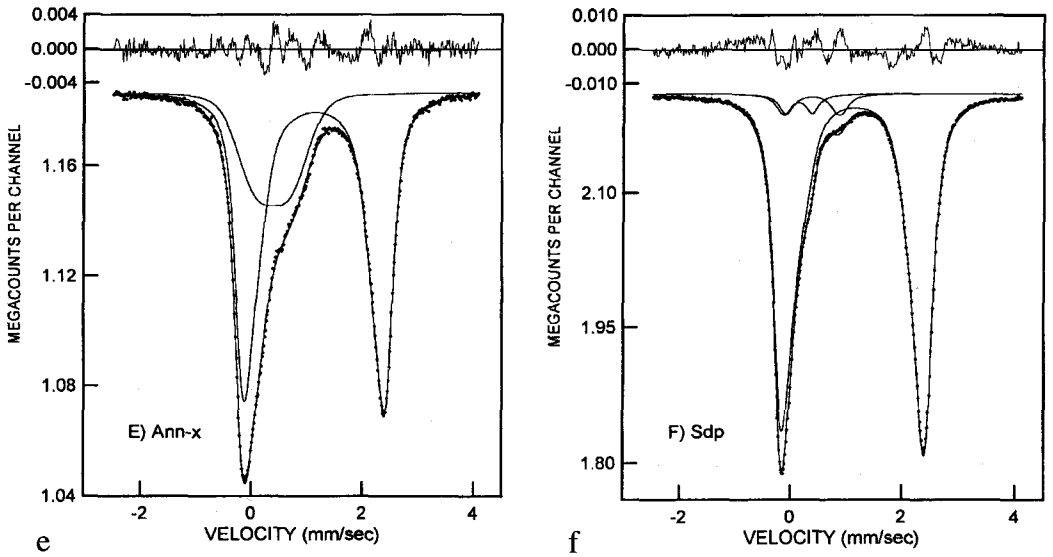

FIG. 2. Mössbauer spectra of Fe-bearing trioctahedral micas from Mont Saint-Hilaire. (*a*) Bt-b, (*b*) Bt-c, (*c*) Bt-d, (*d*) Ann, (*e*) Ann-x, (*f*) Sdp. The solid line running through the spectral data represents the best fit. The subspectral contributions corresponding to $(Fe^{2+})^{vi}$, $(Fe^{3+})^{vi}$ and $(Fe^{3+})^{iv}$ (where resolved) are shown superimposed on the data. The difference spectrum is shown at the top of the figure with an exaggerated vertical scale.

of three Gaussian components (see Rancourt and Ping, 1991). The $(Fe^{3+})^{iv}$ and $(Fe^{3+})^{vi}$ contributions were modelled by QSDs assumed to be composed of single Gaussian components. Fitting parameters for the best fits of all spectra are given in Table 4.

Spectra of specimens from the biotite-annite series (Fig. 2*a*–*e*) show a considerable range of Fe^{3+}/Fe_{tot} from 0.121 (Bt-b) to 0.282 (Ann-x). Errors in these values are always very small, typically $\leqslant 0.005$, demonstrating the robustness of this parameter. In the same specimens, measured values of $(Fe^{3+})^{iv}/Fe_{tot}$ range from 0.066 (Bt-c) to 0.107 (Bt-d) with errors as high as 0.018 (Table 3). The higher errors reflect the inherent problems of overlap between the spectral components of tetrahedral and octahedral Fe^{3+}. The values of $(Fe^{3+})^{iv}/Fe_{tot}$ measured by Mössbauer spectroscopy compare very well with those predicted by site assignments (Table 3). The high proportion of Fe^{3+} in tetrahedral coordination is an outstanding compositional feature of biotite and annite from Mont Saint-Hilaire.

The spectrum of siderophyllite (Fig. 2*f*) is very similar to those of the biotite-annite series and, although iron is less oxidized ($Fe^{3+}/Fe_{tot} = 0.079$), it shows clear spectral components attributed to $(Fe^{2+})^{vi}$, $(Fe^{3+})^{vi}$ and, $(Fe^{3+})^{iv}$. To our knowledge, this is the first Mössbauer spectrum of siderophyllite that shows $(Fe^{3+})^{iv}$.

Mineral chemistry

The mean chemical composition of each of the 8 specimens studied is presented in Table 1 along with its respective structural formula based on 22 oxygen atoms. Titanium was not assigned to tetrahedral sites (Robert, 1976). Calculations of H_2O are based on stoichiometry (i.e. OH+F+Cl = 4). All specimens except Phl and Bt-a have FeO and Fe_2O_3 contents determined by Mössbauer spectroscopy. In addition, specimens Bt-b, -c, -d, Ann and Sdp also have $(Fe^{3+})^{iv}/Fe_{tot}$ determined by Mössbauer spectroscopy.

Phlogopite, biotite and annite. Specimens Phl, Bt-a, -b, -c, -d, Ann and Ann-x are members of the phlogopite-biotite-annite series. On the basis of Mn contents, Ti contents and other compositional characteristics we distinguish amongst these specimens those micas that are representative of the East Hill syenitic rocks (Bt-b, -c, -d, Ann and Ann-x), xenocrystic mica from the earlier gabbroic rocks of the intrusion (Bt-a) and, mica associated with marble xenoliths (Phl). The justification for these three types is given below.

One striking feature of specimens Bt-b, -c, -d, Ann and Ann-x is their high Mn contents. In this group of specimens, Mn ranges from 0.232 to 0.752 atoms per formula unit (a.f.u.). Manganese usually enters biotite through simple substitution for Fe^{2+}, but

TABLE 4. Mössbauer spectrum fitting parameters

FIT	γ	BG	A_{TOT}	δ_0<3^+>	$\delta_0[3^+]$	$\delta_0[2^+]$	$\delta_1[2^+]$	Δ_0<3^+>	σ_Δ<3^+>	$\Delta_0[3^+]$	$\sigma_\Delta[3^+]$	$\Delta_{01}[2^+]$	$\sigma_{\Delta 1}[2^+]$	$\Delta_{02}[2^+]$	$\sigma_{\Delta 2}[2^+]$	$\Delta_{03}[2^+]$	$\sigma_{\Delta 3}[2^+]$	a<3^+>	a[3^+]	$a_1[2^+]$	$a_2[2^+]$	$a_3[2^+]$	$\chi_2$red
Bt-b (1-1-3)	0.2505	839.24	243.71	0.1518	0.4667	1.2044	−0.0328	0.4666	0.0800	0.7463	0.3185	2.6423	0.0674	2.3525	0.1940	1.9620	0.2841	7.54	4.59	28.17	37.08	22.62	1.32
Bt-c (1-1-3)	0.2561	8535.7	1681.7	0.1523	0.4698	1.2516	−0.0496	0.4781	0.0000	0.8004	0.3226	2.6182	0.0857	2.2431	0.3073	1.7054	0.6710	6.60	5.65	31.30	50.68	5.76	5.00
Bt-d (1-1-3)	0.2380	1330.9	420.95	0.2583	0.4306	1.1335	−0.0058	0.3444	0.1814	0.7780	0.4027	2.6263	0.0834	2.3889	0.2356	2.0419	0.4642	10.67	6.08	27.84	41.39	14.01	1.53
Ann (1-1-3)	0.2608	397.09	185.50	0.1899	0.5211	1.2321	−0.0432	0.4522	0.0910	0.7358	0.3729	2.6067	0.0700	2.3113	0.2620	1.7930	0.6100	7.12	10.42	28.36	42.48	11.62	1.20
Ann-x (1-3)	0.2000[1]	1186.4	333.80	–	0.3791	1.1705	−0.0138	–	–	0.6233	0.5833	2.5973	0.1705	2.2334	0.3325	1.8578	1.0671	–	28.19	28.99	32.04	10.78	1.80
Sdp (1-1-3)	0.2780	2208.7	608.36	0.1274	0.3692	1.2527	−0.0500	0.4887	0.0000	0.9957	0.1354	2.6248	0.0608	2.4104	0.1974	1.8544	0.2140	3.36	4.48	34.17	42.98	15.01	5.06

Note: Symmetric doublets are assumed for all sites. The <3^+>, [3^+] and [2^+] refer respectively to $(Fe^{3+})^{iv}$-, $(Fe^{3+})^{vi}$-, and $(Fe^{2+})^{vi}$-specific parameters. Parameters γ, δ_0, Δ_0 and σ_Δ are in mm/s. BG is in kilocounts per channel. The total absorption area, A_{TOT}, is in kilocounts per channel times mm/s. Parameter δ_1 is dimensionless. The site- and component-specific areas (a<3^+>, etc...) are in percentages of A_{TOT}.

[1] This parameter frozen at 0.2000.

rarely exceeds 0.2 a.f.u. (Deer *et al.*, 1962). Many of the exotic minerals of the East Hill suite at Mont Saint-Hilaire are Mn-rich phases, for example, serandite, kupletskite, pyrophanite, and rhodochrosite. Since Mn-enrichment is a compositional characteristic of the East Hill syenites, we consider this group of biotite and annite specimens as primary or postmagmatic phases of the East Hill suite syenites. All specimens are Fe-rich with Fe/(Fe+Mg) between 0.613 to 0.974. Specimens Ann and Ann-x are nearly pure end-member annite. Micas of the East Hill suite are poor in Al. In most specimens total Al is less than 2 a.f.u. This is in part because Al^{iv} contents are low, but also because all samples have practically no Al^{vi} (0 to 0.084 a.f.u.).

Specimen Bt-a is an Mg-rich biotite [Fe/(Fe+Mg) = 0.445], with normal Mn content (0.031 a.f.u.), and very high Ti (0.824 a.f.u.). The Mg-rich nature of this biotite is consistent with its occurrence in a mafic rock-unit. The high Ti content of this mica is a compositional characteristic of biotite from the gabbroic rocks of Mont Saint-Hilaire and of the rocks themselves (see Table 7 in Greenwood and Edgar, 1984). Unlike the biotite and annite from the East Hill suite, specimen Bt-a has higher total Al contents (2.460 a.f.u.), but still requires Fe^{3+} to fill the tetrahedral sites.

Specimen Phl is a phlogopite [Fe/(Fe+Mg) = 0.293] with low Mn and Ti contents (0.041 and 0.015 a.f.u., respectively) and high fluorine (F = 1.556 a.f.u.). The magnesian nature of this mica is consistent with its occurrence in a diopside-rich marble xenolith that occurs within the syenite in the quarry. The specimen has less than 2 a.f.u. of Al, but since Si is higher than all the other micas studied, it does not require Fe^{3+} to fill the tetrahedral sites.

Siderophyllite. Specimen Sdp is a siderophyllite characterized by extreme enrichment in iron [Fe/(Fe+Mg) = 0.975] and aluminum (4.187 a.f.u.). Aluminum is distributed between tetrahedral and octahedral sites (2.873 a.f.u. of Al^{iv} and 1.314 a.f.u. of Al^{vi}). The specimen has very little Ti (0.033 a.f.u.) and high Mn (0.239 a.f.u.). The high Mn content of this mica suggests that the metasomatized albitite dyke in which it occurs is a member of the East Hill suite of syenitic rocks.

Discussion

The alkaline intrusion of Mont Saint-Hilaire is characterized by an overall petrological, mineralogical and geochemical complexity which, not surprisingly, is reflected by the trioctahedral micas of its rocks. In the trioctahedral mica quadrilateral (Fig. 3), two salient features stand out. First, the micas display a wide range of Fe/(Fe+Mg) values, from 0.293 to 0.975. Second, they show an odd bimodal distribution of Al contents; micas either have very little Al (often less than the usual minimum of 2 a.f.u.) or very high abundance of this element (siderophyllite with 4.2 a.f.u. of Al).

The micas show a wide range of Fe/(Fe+Mg) values, but then not all are related to the intrusive rocks. If we disregard the phlogopite which is a metamorphic mineral in the marble xenoliths and focus on the igneous rocks of the intrusion, we observe an increase in Fe/(Fe+Mg) from 0.445 in the gabbro (Bt-a) to 0.975 in the nepheline syenite and albitite (Sdp, Ann and Ann-x). Although iron-enrichment is typical of alkaline rocks, rarely is it so pronounced as at Mont Saint-Hilaire. Not surprisingly, some rocks and their associated micas are also highly enriched in Mn, a siderophile element. Manganese shows a general increase from 0.031 in Bt-a from the gabbro and peaks at 0.752 in Bt-d from the syenite (Fig. 4*a*). From there onwards, Mn drops back to approximately 0.3 a.f.u. in the annite and siderophyllite specimens (Ann, Ann-x, Sdp) suggesting a depletion of Mn in the most-evolved magmas, probably brought about by the crystallization of Mn-rich phases. Titanium contents (Fig. 4*b*) show the reverse of Mn and generally decrease from the micas of the mafic rocks (0.824 a.f.u. in Bt-a, gabbro) to those of the syenites and albitite (0.033 in Sdp).

The micas studied by Mössbauer spectroscopy also show a wide range of Fe^{3+}/Fe_{tot} values, from a low of 0.079 in Sdp to a high of 0.282 in Ann-x, suggesting that redox conditions were far from homogeneous in the various magmas and associated miarolitic cavities where crystallization took place. Of particular interest are the two annite specimens, Ann and Ann-x, which have essentially identical major element compositions but radically different Fe^{3+}/Fe_{tot} values (0.175 *vs.* 0.282, respectively). We originally interpreted Ann-x as a thermally-oxidized equivalent of Ann. However, the lack of any evidence in support of a late thermal metamorphism and the occurrence of Ann-x as euhedral crystals in a young syenite dyke, suggest to the contrary that the high Fe^{3+}/Fe_{tot} value is a primary feature of this mica.

Except for the metamorphic phlogopite and the siderophyllite, the micas studied have Si and Al abundances that are insufficient to fill the tetrahedral sites and thus require $(Fe^{3+})^{iv}$. The presence of $(Fe^{3+})^{iv}$ is confirmed by Mössbauer spectroscopy; spectra of specimens Bt-b, -c, -d, Ann and Sdp all show a distinct shoulder at 0.4 mm/s attributable to $(Fe^{3+})^{iv}$. In these micas, the proportion of Fe^{3+} in tetrahedral coordination varies from 41% (Ann) to 64% (Bt-d). In Ann-x, the Fe^{3+}-rich annite, the spectral contribution of $(Fe^{3+})^{iv}$ is completely overlapped by $(Fe^{3+})^{vi}$.

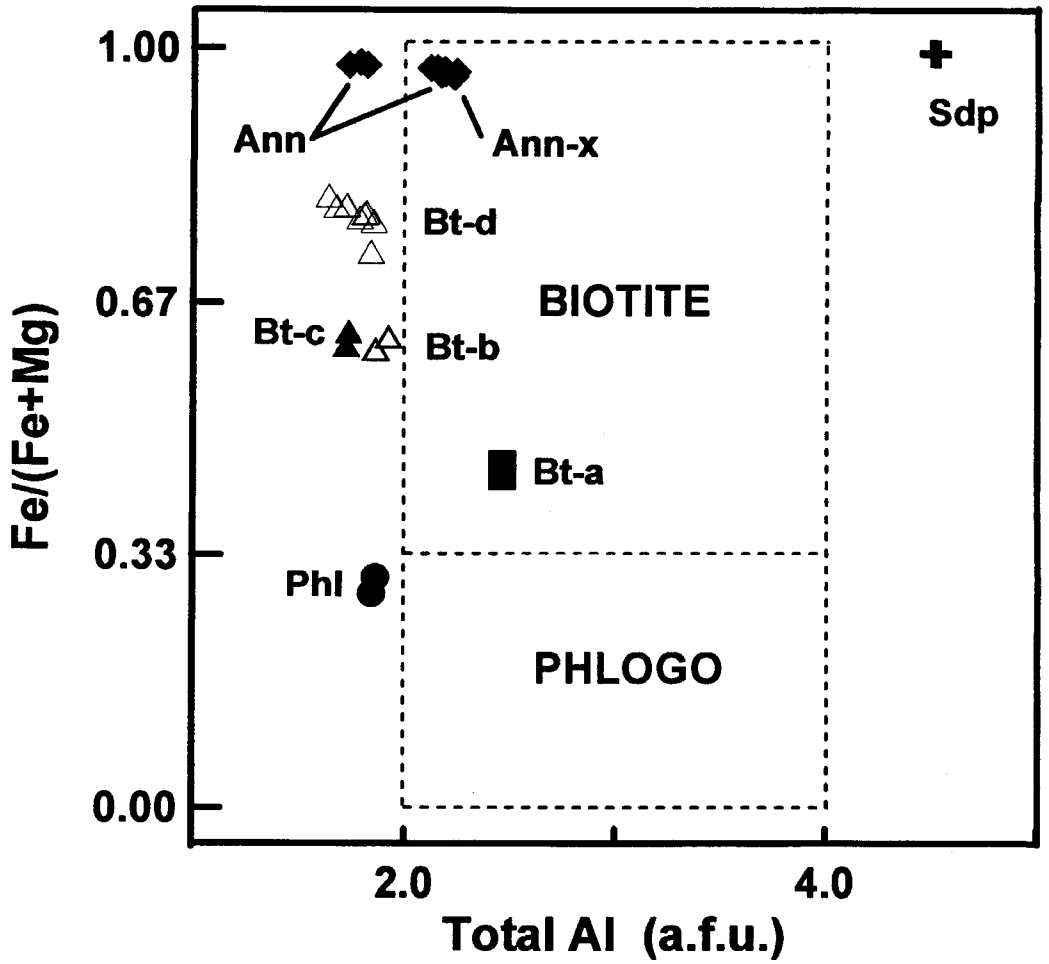

FIG. 3. Plot of Fe/(Fe+Mg) *vs.* total Al (trioctahedral mica quadrilateral) for all the studied micas.

It is not clear why the micas from the igneous rocks at Mont Saint-Hilaire have Fe^{3+} in their tetrahedral sites. The low contents of Al in the biotite and annite specimens is certainly a consequence of the high $(Fe^{3+})^{iv}$ but not the cause of it since siderophyllite, with a total in excess of 4 a.f.u. of Al, still shows a well-defined $(Fe^{3+})^{iv}$ spectral contribution. Since Mn^{2+} is the largest common cation capable of occupying the octahedral sites in micas, one possible explanation is that the high abundance of octahedral Mn^{2+} provokes an expansion of the octahedral sheet which, in turn, compels the tetrahedral sheet to follow by taking in Fe^{3+}, which is also the largest common cation in the tetrahedral sites. The correlation is illustrated in Fig. 5, showing $(Fe^{3+})^{iv}$ a.f.u. *vs.* Mn a.f.u. for all the Fe-bearing micas from the igneous rocks. It is also possible that a more local mechanism is at work, whereby a large Mn^{2+} cation causes a large local distortion that requires Fe^{3+} in neighbouring tetrahedral sites. Indeed, the latter type of mechanism is more likely since the *a* and *b* lattice parameters of Ann are significantly larger than those of Bt-d, showing that the large amount of $(Fe^{3+})^{iv}$ in Bt-d is not simply driven by uniform lateral expansion. Strongly manganoan biotite and phlogopite occur respectively at Mont-Doré in France (Robert and Maury, 1979) and Kamogawa, Japan (Hiroi *et al.* 1992), but at both these localities, $(Fe^{3+})^{iv}$ was not measured by Mössbauer spectroscopy, nor was there a deficiency of Si or Al that would have required Fe^{3+} to fill the tetrahedral sites.

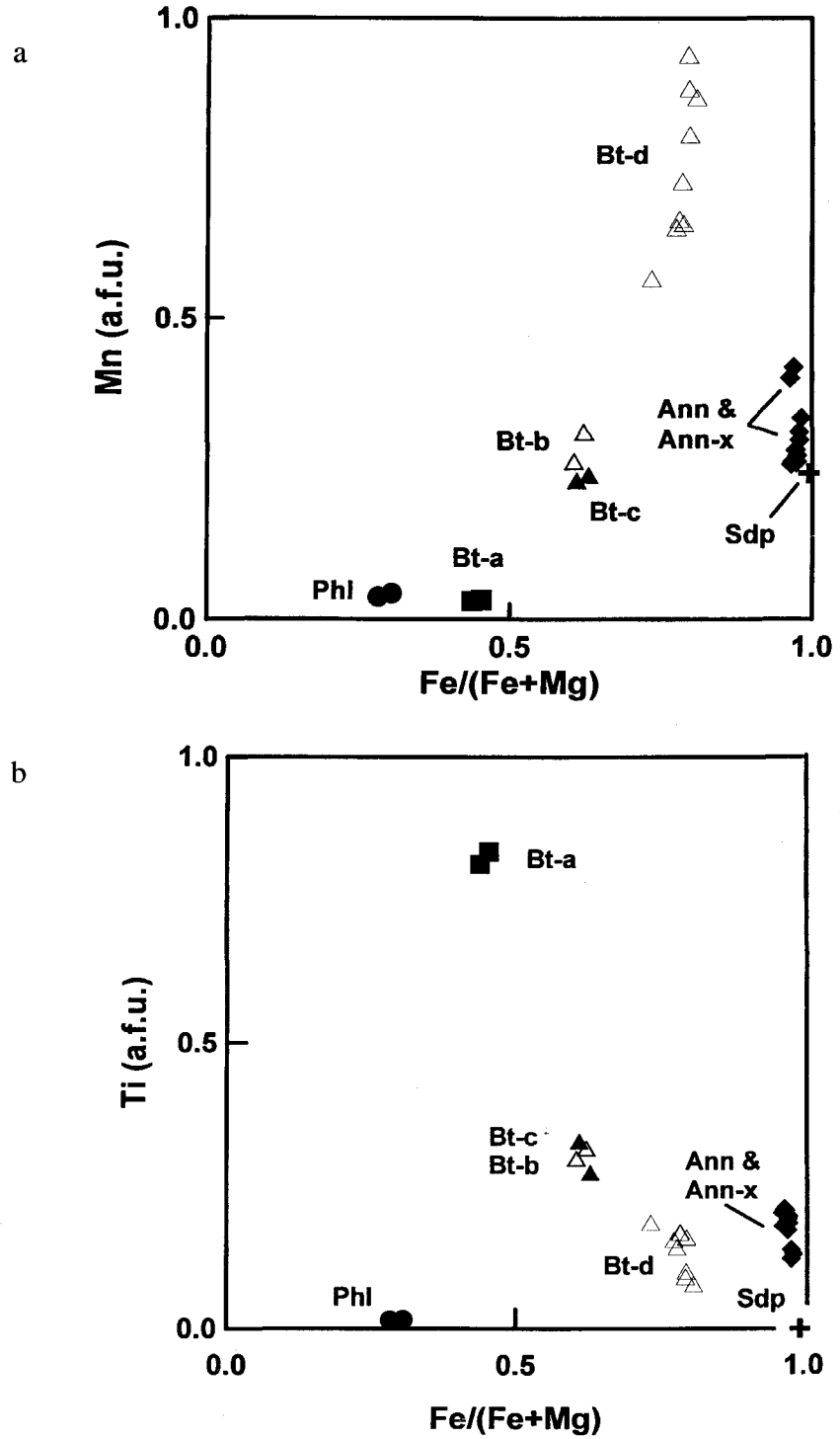

FIG. 4. Plot of Mn (*a*) and Ti (*b*) *vs.* Fe/(Fe+Mg) for the micas of Mont Saint-Hilaire.

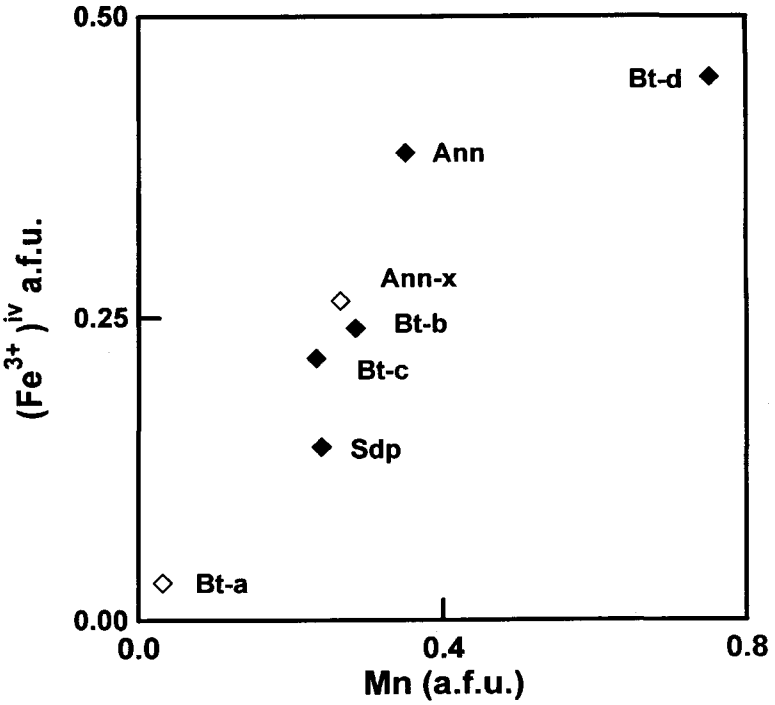

FIG. 5. Plot of $(Fe^{3+})^{iv}$ *vs.* Mn for all the Fe-bearing micas. Solid symbols represent $(Fe^{3+})^{iv}$ values measured by Mössbauer spectroscopy. Hollow symbols are $(Fe^{3+})^{iv}$ values inferred from site assignments.

Siderophyllite at Mont Saint-Hilaire is found as fairly large, mostly subhedral crystals in a late albitite dyke. Although the crystals are interpreted as primary in origin, the chalky-white aphanitic rock in which they occur shows many signs of metasomatism. The term siderophyllite designates aluminian iron-rich biotite. While few mineralogists disagree with this statement, the actual definition of siderophyllite is more controversial. Many formulae and analyses are found in the literature that illustrate a considerable range of total Al contents and Si-Al distributions in the tetrahedral sites. In their text on the sheet silicates, Deer *et al.* (1962) designated siderophyllite with a total of 4 Al a.f.u., as follows:

$$K_2Fe_5Al(Si_5Al_3)O_{20}(OH)_4$$

This is also the formula given by Winchell and Winchell (1951) and by Rutherford (1973) for a synthetic siderophyllite that is the basis of the ICDD card 26-909. Another group of authors, including Levillain *et al.* (1981) and Bailey (1984) attribute a total of 6 Al a.f.u. as follows:

$$K_2Fe_4Al_2(Si_4Al_4)O_{20}(OH)_4$$

This essentially is also the formula given in the *Glossary of Mineral Species* of Fleischer and Mandarino (1991).

Although Levillain *et al.* (1981) did synthesize siderophyllite with a total of 6 Al a.f.u., none of the reported analyses of natural siderophyllites are so aluminian. In the original description of the mineral (Lewis, 1880), the chemical composition when recalculated on the basis of 22 oxygens yields a total of 3.67 Al a.f.u., distributed as follows:

$$Al^{vi}_{1.26}(Si_{5.59}Al_{2.41})$$

Other natural siderophyllites from Brooks Mountain in Alaska (Coats and Fahey, 1944), Mourne Mountains in Northern Ireland (Nockolds and Richey, 1939) and Yagenyama, Japan (Foster, 1960) have total Al contents of 3.01, 4.04, and 4.16 a.f.u., respectively. In our siderophyllite from Mont Saint-Hilaire, there is a total of 4.52 a.f.u. of Al, distributed as follows:

$$Al^{vi}_{1.62}(Si_{4.96}Al_{2.90}Fe^{3+}_{0.14})$$

In view of this, we feel that the idealized formula which is closest to the composition of natural

siderophyllites is:

$$K_2(Fe,Al)_6(Si_{4.5\pm0.5}Al_{3.5\pm0.5})O_{20}(OH)_4.$$

Specimen Sdp, like Ann and Ann-x, is extremely iron-rich [Fe/(Fe+Mg) = 0.975] and it has a high Mn content like all the other micas in the East Hill syenites.

Acknowledgements

We thank Dr J.A. Mandarino for making available sample M29662 from the collection of the Royal Ontario Museum (sample Bt-c in our study). This research was supported by the Natural Sciences and Engineering Research Council of Canada through grants to AEL, DGR and GYC.

References

Adams, F.D. (1903) The Monteregian Hills — A Canadian petrographical province. *J. Geol.*, **11**, 239–82.

Appleman, D.E. and Evans, H.T. Jr. (1973) Job 9214: Indexing and least-squares refinement of powder diffraction data. *United States Geological Survey Computer Contribution* 20.

Bailey, S.W. (1984) Classification and structures of micas. *Reviews in Mineralogy*, **13**, 1–12.

Coats, R.R. and Fahey, J.J. (1944) Siderophyllite from Brooks Mountain, Alaska. *Amer. Mineral.*, **29**, 373–7.

Currie, K.L., Eby, G.N. and Gittins, J. (1986) The petrology of the Mont Saint-Hilaire complex, southern Québec: An alkaline gabbro-peralkaline syenite association. *Lithos*, **19**, 65–81.

Deer, W.A., Howie, R.A. and Zussman J. (1962) *Rock-forming Minerals* **3**. *Sheet Silicates*, Longmans.

Fairbarn, H.W., Faure, G., Pinson, W.H., Hurley, P.M. and Powell, J.L. (1963) Whole rock age and discordant biotite in the Monteregian igneous province, Québec. *J. Geophys. Res.*, **68**, 6515–22.

Fleischer, M. and Mandarino, J.A. (1991) *Glossary of mineral species 1991*. The Mineralogical Record.

Foster, M.D. (1960) Interpretation of the composition of trioctahedral micas. *United States Geological Survey Professional Paper* 354-B.

Gilbert, L.A. and Foland, K.A. (1986) The Mont Saint Hilaire plutonic complex: occurrence of excess ^{40}Ar and short intrusion history. *Canad. J. Earth Sci.*, **23**, 948–58.

Gold, D.P. (1967) Alkaline ultrabasic rocks in the Montréal area, Québec. In: *Ultrabasic related rocks* (P.J.Wyllie, ed.), p. 288–302. John Wiley.

Greenwood, R.C. and Edgar, A.D. (1984) Petrogenesis of the gabbros from Mt. St. Hilaire, Québec, Canada. *Geol. J.*, **19**, 353–76.

Hiroi, Y., Karada-Kondo, H. and Ogo, Y. (1992) Cuprian manganoan phlogopite in highly oxidized Mineoka siliceous schists from Kamogawa, Boso Peninsula, central Japan. *Amer. Mineral.*, **77**, 1099–106.

Horváth, L. and Gault, R.A. (1990) The mineralogy of Mont Saint-Hilaire, Québec. *Mineral. Rec.*, **21**, 284–359.

Kretz, R. (1983) Symbols for rock-forming minerals. *Amer. Mineral.*, **68**, 277–9.

Levillain, C., Maurel, P. and Menil, F. (1981) Mössbauer studies of synthetic and natural micas on the polylithionite-siderophyllite join. *Phys. Chem. Minerals*, **7**, 71–76.

Lewis, H.C. (1880) On siderophyllite - A new mineral. *Proc. Acad. Nat. Sci. Philadelphia*, 254–5.

Mandarino, J.A. and Anderson, V. (1989) *Monteregian Treasures: the Minerals of Mont Saint-Hilaire, Québec*, Cambridge University Press.

Nockolds, S.R. and Richey, J.E. (1939) Replacement veins in the Mourne mountains granites, Northern Ireland. *Amer. J. Sci.*, **237**, 27–47.

Rancourt, D.G. (1989) Accurate site populations from Mössbauer spectroscopy. *Nucl. Inst. Meth. Phys. Res.*, **B44**, 199–210.

Rancourt, D.G. (1994*a*) Mössbauer spectroscopy of minerals. I. Inadequacy of Lorentzian-line doublets in fitting spectra arising from quadrupole splitting distributions. *Phys. Chem. Minerals*, **21**, 244–9.

Rancourt, D.G. (1994*b*) Mössbauer spectroscopy of minerals. II. Problem of resolving cis and trans octahedral Fe^{2+} sites. *Phys. Chem. Minerals*, **21**, 250–7.

Rancourt, D.G. and Ping, J.Y. (1991) Voigt-based methods for arbitrary-shape static hyperfine parameter distributions in Mössbauer spectroscopy. *Nucl. Inst. Meth. Phys. Res.*, **B53**, 85–97.

Rancourt, D.G, Dang, M.-Z. and Lalonde, A.E. (1992) Mössbauer spectroscopy of tetrahedral Fe^{3+} in trioctahedral micas. *Amer. Mineral.*, **77**, 34–43.

Rancourt, D.G., McDonald, A.M., Lalonde, A.E. and Ping, J.Y. (1993) Mössbauer absorber thicknesses for accurate site populations in Fe-bearing minerals. *Amer. Mineral.*, **78**, 1–7.

Rancourt, D.G., Christie, I.A.D., Lamarche, G., Swainson, I. and Flandrois, S. (1994*a*) Magnetism of synthetic and natural annite mica: Ground state and nature of excitations in an exchange-wise two-dimensional easy-plane ferromagnet. *J. Magnetism and Magnetic Materials*, **138**, 31–44.

Rancourt, D.G., Ping, J.Y. and Berman, R.G. (1994*b*) Mössbauer spectroscopy of minerals. III. Octahedral-site Fe^{2+} quadrupole splitting distributions in the phlogopite-annite series. *Phys. Chem. Minerals*, **21**, 258–67.

Rancourt, D.G., Christie, I.A.D., Royer, M., Kodama, H., Robert, J.-L., Lalonde, A.E. and Murad, E. (1994*c*) Determination of accurate $^{[4]}Fe^{3+}$, $^{[6]}Fe^{3+}$,

$^{[6]}Fe^{2+}$ site populations in synthetic annite by Mössbauer spectroscopy. *Amer. Mineral.*, **79**, 51–62.

Robert, J.-L. (1976) Titanium solubility in synthetic phlogopite solid solutions. *Chem. Geol.*, **17**, 213–27.

Robert, J.-L. and Maury, R.C. (1979) Natural occurrence of a (Fe, Mn, Mg) tetrasilicic potassium mica. *Contrib. Mineral. Petrol.*, **68**, 117–23.

Rutherford, M.J. (1973) The phase relations of aluminous iron biotites in the system $KAlSi_3O_8$–$KAlSiO_4$–Al_2O_3–Fe–O–H. *J. Petrol.*, **14**, 159–80.

Winchell, A.N. and Winchell, H. (1951) *Elements of Optical Mineralogy, part 2*. John Wiley and Sons.

[*Manuscript received 23 August 1994: revised 30 January 1995*]